



1 **Evidence of cryptic methane cycling and non-methanogenic**
2 **methylamine consumption in the sulfate-reducing zone of**
3 **sediment in the Santa Barbara Basin, California**

4 Sebastian J.E. Krause^{1*#}, Jiarui Liu¹, David J. Yousavich¹, DeMarcus Robinson², David W.
5 Hoyt³, Qianhui Qin⁴, Frank Wenzhoefer^{5,6,7}, Felix Janßen^{5,6}, David L. Valentine⁸, and Tina
6 Treude^{1,2*}

7 ¹Department of Earth Planetary and Space Sciences, University of California, Los Angeles, CA
8 90095, USA

9 ²Department of Atmospheric and Ocean Sciences, University of California, Los Angeles, CA
10 90095, USA

11 ³Pacific Northwest National Laboratory Environmental and Molecular Sciences Division,
12 Richland, WA 99352, USA

13 ⁴Interdepartmental Graduate Program in Marine Science, University of California, Santa
14 Barbara, CA 93106, USA

15 ⁵HGF-MPG Group for Deep-Sea Ecology and Technology, Alfred-Wegener-Institute,
16 Helmholtz-Center for Polar and Marine Research, Am Handelshafen 12, 27570 Bremerhaven,
17 Germany

18 ⁶Max Planck Institute for Marine Microbiology, Celsiusstrasse 1, 28359 Bremen, Germany

19 ⁷Department of Biology, DIAS, Nordcee and HADAL Centres, University of Southern
20 Denmark, 5230 Odense M, Denmark

21 ⁸Department of Earth Science and Marine Science Institute, University of California Santa
22 Barbara, Santa Barbara, CA 93106, USA

23 *Correspondence: Sebastian Krause (sjkrause@ucsb.edu), Tina Treude (ttreude@g.ucla.edu)

<https://doi.org/10.5194/egusphere-2023-909>

Preprint. Discussion started: 8 May 2023

© Author(s) 2023. CC BY 4.0 License.



24 **# Present address: Earth Research Institute, 6832 Ellison Hall, University of California**

25 **Santa Barbara, Ca 93106-3060**



26 **Abstract.** The recently discovered cryptic methane cycle in the sulfate-reducing zone of marine
27 and wetland sediments couples methylotrophic methanogenesis to anaerobic oxidation of
28 methane (AOM). Here we present evidence of cryptic methane cycling activity within the
29 upper regions of the sulfate-reducing zone, along a depth transect within the Santa Barbara
30 Basin, off the coast of California, USA. The top 0-20 cm of sediment from each station was
31 subjected to geochemical analyses and radiotracer incubations using $^{35}\text{S-SO}_4^{2-}$, ^{14}C -mono-
32 methylamine, and $^{14}\text{C-CH}_4$ to find evidence of cryptic methane cycling. Methane
33 concentrations were consistently low (~ 3 to ~ 16 μM) across the depth transect, despite AOM
34 rates increasing with decreasing water depth (from max 0.05 $\text{nmol cm}^{-3} \text{d}^{-1}$ at the deepest station
35 to max 1.8 $\text{nmol cm}^{-3} \text{d}^{-1}$ at the shallowest station). Porewater sulfate concentrations remained
36 high (~ 23 mM to ~ 29 mM), despite the detection of sulfate reduction activity from $^{35}\text{S-SO}_4^{2-}$
37 incubations with rates up to 134 $\text{nmol cm}^{-3} \text{d}^{-1}$. Metabolomic analysis showed that substrates
38 for methanogenesis (i.e., acetate, methanol and methylamines) were mostly below the detection
39 limit in the porewater, but some samples from the 1-2 cm depth section showed non-
40 quantifiable evidence of these substrates, indicating their rapid turnover. Estimated
41 methanogenesis from mono-methylamine ranged from 0.2 nmol to 0.5 $\text{nmol cm}^{-3} \text{d}^{-1}$.
42 Discrepancies between the rate constants (K_1) of methanogenesis (from ^{14}C - mono-
43 methylamine) and AOM (from either ^{14}C - mono-methylamine-derived $^{14}\text{C-CH}_4$ or from
44 directly injected $^{14}\text{C-CH}_4$) suggest the activity of a separate, concurrent metabolic process
45 directly metabolizing mono-methylamine to inorganic carbon. We conclude that the results
46 presented in this work show strong evidence of cryptic methane cycling occurring within the
47 top 20 cm of sediment in the Santa Barbara Basin. The rapid cycling of carbon between
48 methanogenesis and methanotrophy likely prevents major build-up of methane in the sulfate-
49 reducing zone. Furthermore, our data suggest that methylamine is utilized by both
50 methanogenic archaea capable of methylotrophic methanogenesis and non-methanogenic



51 microbial groups. We hypothesize that sulfate reduction is responsible for the additional
52 methylamine turnover but further investigation is needed to elucidate this metabolic activity.
53



54 **1. Introduction**

55 In anoxic marine sediment, methane is produced by microbial methanogenesis in the
56 last step of organic carbon remineralization (Stephenson and Stickland, 1933; Thauer, 1998;
57 Reeburgh, 2007). This methane is produced by groups of obligate anaerobic methanogenic
58 archaea across the Euryarchyota, Crenarchaeota, Halobacterota, and Thermoplasmata phyla
59 (Lyu et al., 2018). Methanogens can produce methane through three different metabolic
60 pathways, using CO₂ (CO₂ reduction; e.g., hydrogenotrophic) (Eq. 1), acetate (acetoclastic)
61 (Eq. 2) and methylated substrates such as, methyl sulfides, methanol, and methylamines
62 (methylotrophic) (e.g., Eq. 3).

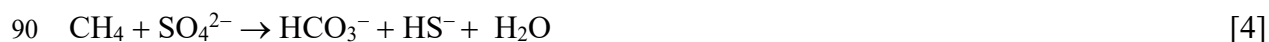


66 Classically, hydrogenotrophic and acetoclastic methanogenesis are dominant in deeper
67 sulfate-free sediment (Jørgensen, 2000; Reeburgh, 2007). This distinct geochemical zonation
68 is due to the higher free energy gained by sulfate-reducing bacteria within the sulfate reduction
69 zone coupling sulfate reduction with hydrogen and/or acetate consumption in sulfate-rich
70 sediment. Thus, sulfate-reducing bacteria tend to outcompete methanogenic archaea for
71 hydrogen and acetate in shallower sediment layers in the presence of sulfate (Kristjansson et
72 al., 1982; Winfrey and Ward, 1983; Lovley and Klug, 1986; Jørgensen, 2000). However,
73 methylotrophic methanogenesis is known to occur within the sulfate-reducing zone. The
74 activity of this process in the presence of sulfate reduction is possible because methylated
75 substrates, such as methylamines, are non-competitive carbon sources for methanogens
76 (Oremland and Taylor, 1978; Lovley and Klug, 1986; Maltby et al., 2016; Zhuang et al., 2016;
77 2018; 2018; Krause and Treude, 2021). Methylotrophic methanogenesis activity in the sulfate-
78 reducing zone has been detected in a wide range of aquatic environments, such as coastal
79 wetlands (Oremland et al., 1982; Oremland and Polcin, 1982; Krause and Treude, 2021),



80 upwelling regions (Maltby et al., 2016), and eutrophic shelf sediment (Maltby et al., 2018; Xiao
81 et al., 2018). Despite methylophilic activity in the sulfate-reducing zone, methane
82 concentrations are several orders of magnitude lower than methane concentrations found in
83 deeper sediment zones where sulfate concentrations are depleted (Barnes and Goldberg, 1976;
84 Dale et al., 2008b; Wehrmann et al., 2011; Beulig et al., 2018).

85 In anoxic marine sediment, anaerobic oxidation of methane (AOM) is an important
86 methane sink that is typically coupled to sulfate reduction (Eq. 4) and mediated by a consortium
87 of anaerobic methane-oxidizing archaea (ANME) and sulfate-reducing bacteria (Knittel and
88 Boetius, 2009; Orphan et al., 2001; Michaelis et al., 2002; Boetius et al., 2000; Hinrichs and
89 Boetius, 2002; Reeburgh, 2007).



91 AOM occurring in the sulfate-reducing zone, fuelled by concurrent methylophilic
92 methanogenesis activity, i.e., the cryptic methane cycle, could be the reason why methane
93 concentrations are consistently low in sulfidic sediment (Krause and Treude, 2021; Xiao et al.,
94 2017; Xiao et al., 2018). These studies highlight the importance of the cryptic methane cycle
95 on the global methane budget. However, the extent of our knowledge of cryptic methane cycle
96 is restricted to a few aquatic environments. Thus, it is crucial to investigate and understand the
97 cryptic methane cycle in myriad environments to fully understand its impact on the global
98 methane budget. In the present study we focus on organic-rich sediment below oxygen-
99 deficient water in the Santa Barbara Basin (SSB), California.

100 Oxygen minimum zones (OMZ) are regions where high oxygen demand in the water
101 column leads to a dramatic decline or even absence of dissolved oxygen (Wright et al., 2012;
102 Paulmier and Ruiz-Pino, 2009; Wyrski, 1962; Canfield and Kraft, 2022). In these
103 environments, coastal upwelling of nutrients results in high phytoplankton growth, greatly
104 enhancing organic matter loading and in turn creating a high metabolic oxygen demand during
105 organic matter degradation in the water column. This enhanced respiration depletes oxygen



106 faster than it is replenished (especially in poorly ventilated water bodies), which results in
107 strong seasonal or continuous low oxygen conditions (Wyrski, 1962; Helly and Levin, 2004;
108 Wright et al., 2012; Levin et al., 2009). Sediment beneath OMZs is typically rich in organic
109 matter supporting predominantly or exclusively anaerobic degradation processes, including
110 methanogenesis (Levin, 2003; Rullkötter, 2006; Middelburg and Levin, 2009; Fernandes et al.,
111 2022; Treude, 2011). Thus, sediments underlying OMZ's are good candidate environments to
112 investigate cryptic methane cycling.

113 Located within the Pacific Ocean, between the Channel Islands and the mainland of
114 Santa Barbara, California, USA, the SBB is characterized as a thermally stratified, coastal
115 marine basin with a maximum water column depth of approximately 590 m (Soutar and Crill,
116 1977; Arndt et al., 1990; Sholkovitz, 1973). Low oxygen concentrations ($<10 \mu\text{M}$) are found
117 in the bottom waters below the sill depth ($\sim 475 \text{ m}$) of the SBB (Sholkovitz, 1973; Reimers et
118 al., 1996). The sediment in the SBB have an organic carbon content between 2-6%
119 (Schimmelmann and Kastner, 1993). These characteristics makes the SBB a prime study site
120 to find evidence of cryptic methane cycling.

121 Organic carbon sources for methylotrophic methanogenesis, such as methylamine, are
122 ubiquitous in the coastal marine environments (Zhuang et al., 2018; Zhuang et al., 2016; Oren,
123 1990), including marine environments where OMZ's exist (Ferdelman et al., 1997; Gibb et al.,
124 1999). Methylamines are derived from osmolytes, such as glycine and betaine, and are
125 synthesized by phytoplankton (Oren, 1990). However, the abundance of methylamines and
126 how they may be driving cryptic methane cycling in anoxic sediment within OMZ's are
127 virtually unknown. Furthermore, the fate of methane from methylotrophic methanogenesis in
128 the sulfate reduction zone is poorly constrained. Particularly, if cryptic methane cycling is
129 active above the sulfate-methane transition zone, gross production and consumption of
130 methane have likely been underestimated. Therefore, finding evidence for the cryptic methane



131 cycle in the SBB is a necessary step towards understanding how carbon is cycled through the
132 sediment of the SBB and other OMZs.

133 In the present study we report biogeochemical evidence of cryptic methane cycling in
134 surface sediment (top ~15 cm) collected along a depth transect crossing the SBB. We applied
135 the radiotracer method from Krause and Treude (2021) to trace the production of methane from
136 mono-methylamine, followed by the anaerobic oxidation of methane to inorganic carbon. We
137 combined this approach with standard radiotracer methods for the detection of AOM and
138 sulfate reduction as well as with analyses of sediment porewater geochemistry.

139



140 **2. Methods.**

141 **2.1. Study site and sediment sampling**

142 Sediment samples were collected during the R/V *Atlantis* expedition AT42-19 in fall
143 2019. Collection was achieved with polycarbonate push cores (30.5 cm long, 6.35 cm i.d.),
144 which were deployed by the ROV *JASON* along a depth transect through the SBB. The depth
145 transect selected for this particular study, was the Northern Deposition Transect 3 (NDT3),
146 with three stations (NDT3-A, -C and -D), as well as the Northern Depositional Radial Origin
147 (NDRO), and the Southern Depositional Radial Origin (SDRO) station, located in the deepest
148 part of the basin. Details on the station's water column depths and near-seafloor oxygen
149 concentrations are provided in Table 1.

150 **Table 1.** Water column depth, bottom water oxygen concentrations and coordinates of each station sampled during
151 this study.

Station	Depth (m)	Bottom Water Oxygen (μM)	Latitude	Longitude
SDRO	586	0	34.2011	-120.0446
NDRO	580	0	34.2618	-120.0309
NDT3-A	572	9.2	34.2921	-120.0258
NDT3-C	498	5	34.3526	-120.0160
NDT3-D	447	8	34.3625	-120.0150

152
153 After sediment collection, ROV push cores were returned to the surface by an elevator
154 platform. Upon retrieval onboard the R/V *Atlantis*, sediment samples were immediately
155 transported to an onboard cold room (6°C) for further processing of biogeochemical parameters
156 (see details in section 2.2.).

157

158 **2.2. Sediment porewater sampling and sulfate analysis**

159 For porewater analyses, two ROV sediment push cores from each station were sliced
160 in 1-cm increments in the top 10 cm of the sediment, followed by 2-cm increments below.



161 During sediment sampling, ultra-pure argon was flushed over the sediment to minimize
162 oxidation of oxygen sensitive species. The sliced sediment layers were quickly transferred to
163 argon-flushed 50 mL plastic centrifuge vials and centrifuged at 2300 X g for 20 mins to extract
164 the porewater. Subsequently, 2 mL of porewater was subsampled from the supernatant and
165 frozen at -20 °C for shore-based sulfate analysis by ion chromatography (Metrohm 761)
166 following (Dale et al., 2015). Additional porewater (1 mL) was subsampled for the
167 determination of the concentration of methylamine and other metabolic substrates (see section
168 2.4).

169

170 ***2.3. Sediment methane and benthic methane flux analyses***

171 Methane concentration in the sediment was determined from a replicate ROV pushcore.
172 Sediment was sliced at 1-cm increments in the top 10 cm, followed by 2-cm increments below.
173 Two mL of sediment was sampled with a cut-off 3 mL plastic syringe and quickly transferred
174 to 12 mL glass serum vials filled with 5 mL 5% (w/w) NaOH solution. The vials were sealed
175 immediately with a grey butyl rubber stopper and aluminum crimps, shaken thoroughly, and
176 stored upside down at 4 °C. Methane concentrations in the headspace were determined shore-
177 based using a gas chromatograph (Shimadzu GC-2015) equipped with a packed Haysep-D
178 column and flame ionization detector. The column was filled with helium as a carrier gas,
179 flowing at 12 mL per minute and heated to 80 °C. Methane concentrations in the environmental
180 samples were calibrated against methane standards (Scotty Analyzed Gases) with a \pm 5%
181 precision.

182 To determine methane flux out of the sediment and into the water column, 1-2
183 custom-built cylindrical benthic flux chambers (BFC) (Treude et al., 2009) were deployed at
184 each sampling station by the ROV Jason. The BFCs consist of a lightweight fiber-reinforced
185 plastic frame, which holds a cylindrical polycarbonate chamber. Buoyant syntactic foam was
186 attached to the feet of the frame to keep the BFC's from sinking too deep into the soft and



187 poorly consolidated sediments, especially in the deeper stations. Water overlying the
188 enclosed sediment was kept mixed with a stirrer bar rotating below the lid of the chamber.
189 The BFC's were equipped with a syringe sampler holding 7, 60 mL glass syringes (6 syringes
190 for sample collection and 1 syringe for freshwater injection). One sample syringe withdrew
191 50 mL of seawater from the chamber volume at pre-programed time intervals. The seventh
192 syringe was used to inject 50 mL of de-ionized water into the chamber shortly after
193 deployment to calculate the volume from the change in salinity in the overlying seawater
194 recorded by a conductivity sensor (type 5860, Aanderaa Data Instruments, Bergen, NO),
195 according to (Kononets et al., 2021).

196 Prior to BFC seawater sample collection, the 26 mL serum bottles were acid washed,
197 rinsed three times using MilliQ filtered DI water, and then combusted at 300 °C. One to two
198 pellets of solid NaOH were added into each empty combusted serum bottle. All empty serum
199 bottles were then flushed with ultra-pure nitrogen gas (Airgas Ultra High Purity Grade
200 Nitrogen, Manufacturer Part #:UHP300) for 5 min, then sealed with autoclaved chlorobutyl
201 stoppers and crimps. Lastly, a vacuum pump was used to evacuate the bottles to a pressure
202 down to <0.05 psi prior to sample collection.

203 Immediately after BFC recovery from the seafloor, approximately 20 mL of seawater
204 sample was transferred into the pre-evacuated 26 mL glass serum bottles through the
205 chlorobutyl stopper using a sterile 23G needle. Pressure within the serum bottle was
206 equalized to atmospheric pressure with the introduction of UHP grade nitrogen. Serum
207 bottles were shaken to dilute the NaOH pellets, which terminated metabolic activity and
208 forced the dissolved methane into the gas headspace. The serum bottles were reweighed after
209 sample collection, to calculate the exact volume of the seawater sample. Methane
210 concentrations in seawater collected from the BFC's were analyzed shipboard by gas
211 chromatography according to Qin et al., 2022.



212 Total methane concentration in the headspace was calculated following the ideal gas
213 law Eq. (5),

$$214 \quad n = \frac{PV}{RT} * [CH_4] * \frac{1}{V_{SW}} \quad . \quad [5]$$

215 Where n is the total molar concentration of methane, P is atmospheric pressure, V is the volume
216 of the headspace of serum bottle (which is calculated by 26 mL subtracted by the volume of
217 seawater sample), R is the ideal gas constant, T is temperature in Kelvin (288.15 K), $[CH_4]$ is
218 the methane measured by GC as percentage values in ppm, and V_{SW} is the volume of seawater
219 in the serum vial. The volume of sampled seawater in each serum bottle was calculated by
220 subtracting the mass of the empty serum bottle from the mass of the filled serum bottle,
221 normalized by the density of seawater.

222

223 **2.4. Porewater metabolomic analysis**

224 To obtain sediment porewater concentrations of methanogenic substrates
225 (methylamine, methanol, and acetate), 1 mL porewater was extracted from 1-2 cm and 9-10
226 cm depth sections at each station (see section 2.2) and syringe-filtered (0.2 μ m) into pre-
227 combusted (350 °C for 3 hrs) amber glass vials (1.8 mL), which were then closed with a PTFE
228 septa-equipped screw caps and frozen at -80 °C until analyses. Samples were analysed at the
229 Pacific Northwest National Laboratory, Environment and Molecular Sciences Division for
230 metabolomic analysis using proton nuclear magnetic resonance (NMR). Prior to analysis,
231 porewater samples were diluted by 10% (v/v) with an internal standard (5 mM 2,2-dimethyl-
232 2-silapentane-5-sulfonate-d6). All NMR spectra were collected using an 800 MHz Bruker
233 Avance Neo (Tava), with a TCI 800/54 H&F/C/N-D-05 Z XT, and an QCI H-P/C/N-D-05 Z
234 ET extended temperature range CryoProbe. The 1D ¹H NMR spectra of all samples were
235 processed, assigned, and analysed by using the Chenomx NMR Suite 8.6 software with
236 quantification based on spectral intensities relative to the internal standard. Candidate
237 metabolites present in each of the complex mixture were determined by matching the chemical



238 shift, J-coupling, and intensity information of experimental NMR signals against the NMR
239 signals of standard metabolites in the Chenomx library. The 1D ^1H spectra were collected
240 following standard Chenomx data collection guidelines, employing a 1D NOESY presaturation
241 experiment (noesypr1d) with 65536 complex points and at least 4096 scans at 298 K. Signal to
242 noise ratios (S/N) were measured using MestReNova 14 with the limit of quantification equal
243 to a S/N of 10 and the limit of detection equal to a S/N of 3. The 90° ^1H pulse was calibrated
244 prior to the measurement of each sample with a spectral width of 12 ppm and 1024 transients.
245 The NOESY mixing time was 100 ms and the acquisition time was 4 s followed by a relaxation
246 delay of 1.5 s during which presaturation of the water signal was applied. Time domain free
247 induction decays (72114 total points) were zero-filled to 131072 total points prior to Fourier
248 transform.

249

250 ***2.5. Metabolic activity determinations***

251 One replicate ROV sediment push core (hereafter 'ROV rate push core') from each
252 station was sub-sampled with three mini-cores (20 cm long, 2.6 cm i.d.) for radiotracer
253 incubations according to the whole-core injection method (Jørgensen 1978) to collect
254 quantitative metabolic evidence (sulfate reduction, methanogenesis, methane oxidation) of
255 cryptic methane cycling. The incubation methods are detailed below.

256

257 ***2.5.1. Sulfate reduction via ^{35}S -Sulfate***

258 Within the same day of collection, one mini-core from each ROV rate push core was
259 used to determine sulfate-reduction rates. Radioactive carrier-free ^{35}S -sulfate ($^{35}\text{S}\text{-SO}_4^{2-}$;
260 dissolved in MilliQ water, injection volume 10 μL , activity 260 KBq, specific activity 1.59
261 TBq mg^{-1}) was injected into the mini core at 1-cm increments and incubated at 6°C in the dark
262 following (Jørgensen, 1978). Injected sediment cores were stored vertically and incubated for
263 ~ 6 hrs at 6°C in the dark. Incubations were stopped by slicing the sediment in 1-cm increments



264 into 50 mL plastic centrifuge tubes containing 20 mL 20% (w/w) zinc acetate solution. Each
265 sediment sample was sealed and shaken thoroughly and stored at -20 °C to halt metabolic
266 activity. For the control samples, sediments were added to zinc acetate solution prior to
267 radiotracer injection. In the home laboratory, sulfate reduction rates were determined using the
268 cold-chromium distillation method (Kallmeyer et al., (2004).

269

270 ***2.5.2. Methanogenesis and AOM via ¹⁴C-Mono-Methylamine***

271 This study aimed at determining the activity of methanogenesis from mono-
272 methylamine (MG-MMA) and the subsequent anaerobic oxidation of the resulting methane to
273 inorganic carbon by AOM (AOM-MMA). To accomplish this goal, a mini core from each ROV
274 rate push core was injected with radiolabeled ¹⁴C-mono-methylamine (¹⁴C-MMA; dissolved in
275 1 mL water, injection volume 10 μL, activity 220 KBq, specific activity 1.85-2.22 GBq mmol⁻¹
276 ¹) similar to section 2.5.1. After 24 hrs, the incubation was terminated by slicing the sediment
277 at 1-cm increments into 50 mL wide mouth glass vials filled with 20 mL of 5% NaOH. Five
278 killed control samples were prepared by transferring approximately 5 ml of extra sediment
279 from each station into 50 mL wide mouth vials filled with 20 mL of 5% NaOH prior to
280 radiotracer addition. Sample vials and vials with killed controls were immediately sealed with
281 butyl rubber stoppers and aluminium crimps and shaken thoroughly for 1 min to ensure
282 complete biological inactivity. Vials were stored upside down at room temperature until further
283 processing. In the home laboratory, methane production from ¹⁴C-MMA by MG-MMA and
284 subsequent oxidation of the produced ¹⁴C-methane (¹⁴C-CH₄) by AOM-MMA was determined
285 according to the adapted radiotracer method outlined in (Krause and Treude, 2021).

286 To account for ¹⁴C-MMA potentially bound to mineral surfaces (Wang and Lee, 1993,
287 1994; Xiao et al., 2022), we determined the ¹⁴C-MMA recovery factor (RF) for the sediment
288 from the stations NDT3-C, D and NDRO according to Krause and Treude (2021).



289 Metabolic rates of MG-MMA were calculated according to Eq. 8. Note that natural
290 concentrations of MMA in the SBB sediment porewater were either below detection or
291 detectable, but below the quantification limit (<10 μM) (Table S1). Therefore, MMA
292 concentrations were assumed to be 3 μM to calculate the ex-situ rate of MG-MMA (Eq. 8).

$$293 \quad MG-MMA = \frac{a_{CH_4} + a_{TIC}}{a_{CH_4} + a_{TIC} + \left[\frac{a_{MMA}}{RF}\right]} * [MMA] * \frac{1}{t} \quad [7]$$

294 where *MG-MMA* is the rate of methanogenesis from mono-methylamine ($\text{nmol cm}^{-3} \text{d}^{-1}$); a_{CH_4}
295 is the radioactive methane produced from methanogenesis (CPM); a_{TIC} is the radioactive total
296 inorganic carbon produced from the oxidation of methane (CPM); a_{MMA} the residual
297 radioactive mono-methylamine (CPM); RF is the recovery factor (Krause and Treude, (2021)
298 ; $[MMA]$ is the assumed mono-methylamine concentrations in the sediment (nmol cm^{-3}); t is
299 the incubation time (d). $^{14}\text{C-CH}_4$ and $^{14}\text{C-TIC}$ sample activity was corrected by respective
300 abiotic activity determined in killed controls.

301 Results from the $^{14}\text{C-MMA}$ incubations were also used to estimate the AOM-MMA
302 rates according to Eq. 8,

$$303 \quad AOM-MMA = \frac{a_{TIC}}{a_{CH_4} + a_{TIC}} * [CH_4] * \frac{1}{t} \quad [8]$$

304 where *AOM-MMA* is the rate of anaerobic oxidation of methane based on methane produced
305 from MMA ($\text{nmol cm}^{-3} \text{d}^{-1}$); a_{TIC} is the produced radioactive total inorganic carbon (CPM); a_{CH_4}
306 is the residual radioactive methane (CPM); $[CH_4]$ is the sediment methane concentration (nmol
307 cm^{-3}); t is the incubation time (d). $^{14}\text{C-TIC}$ activity was corrected by abiotic activity determined
308 by replicate dead controls.

309

310 **2.5.3 Anaerobic oxidation of methane via $^{14}\text{C-Methane}$**

311 AOM rates from $^{14}\text{C-CH}_4$ (AOM- CH_4) were determined by injecting radiolabeled $^{14}\text{C-}$
312 CH_4 (dissolved in anoxic MilliQ, injection volume 10 μL , activity 5 KBq, specific activity
313 1.85–2.22 GBq mmol^{-1}) into one mini core from each ROV rate core at 1-cm increments similar



314 to section 2.5.1. Incubations of the mini cores were stopped after ~24 hours similar to section
315 2.5.2. In the laboratory, AOM-CH₄ was analysed using oven combustion (Treude et al., 2005)
316 and acidification/shaking (Joye et al., 2004). The radioactivity was determined by liquid
317 scintillation counting. AOM-CH₄ rates were calculated according to Eq. 8.

318

319 **2.5.4 Rate constants for AOM-CH₄, MG-MMA, and AOM-MMA**

320 Metabolic rate constants (k) for AOM-CH₄, MG-MMA and AOM-MMA were
321 calculated using the experimental data determined by sections 2.5.2 and 2.5.3. The rate
322 constants consider the metabolic reaction products, divided by the sum of reaction reactants
323 and products and by time. The metabolic rate constants for AOM-CH₄, MG-MMA and AOM-
324 MMA were calculated according to Eq. 9,

$$325 \quad k = \frac{a_{products}}{a_{products} + a_{reactants}} * \frac{1}{t} \quad [9]$$

326 where k is the metabolic rate constant (day⁻¹); $a_{products}$ is the radioactivity (CPM) of the
327 metabolic reaction products; $a_{reactants}$ is the radioactivity (CPM) of the metabolic reaction
328 reactants; t is time in days.

329



330 **3. Results**

331 **3.1. Sediment biogeochemistry**

332 At most stations, porewater methane concentrations in the top 10-20 cm of sediment
333 fluctuated between 3 and 13 μM with no clear trend (Fig. 1A, E, I, M, and Q). At NDRO,
334 methane steadily increased below 12 cm, reaching 16 μM at 14–15 cm (Fig. 1E). Methane
335 concentrations determined in water samples from the BFC incubations revealed only minor
336 fluctuations over time with no clear trends suggesting no net fluxes of methane into or out of
337 the sediment at all stations (Fig. 1S). It is notable, however, that the BFCs captured higher
338 methane concentrations (350-800 nM) in the supernatant of station SDRO, NDRO, and NDT3-
339 A compared to NDT3-C and NDT3-D (< 130 nM). Sulfate concentrations showed no strong
340 decline with depth at any station (except maybe a weak tendency at SDRO and NDT3-A) and
341 fluctuated between 23 and 30 mM in the sampled top 10-20 cm (Fig. 1A, E, I, M, and Q).

342 Table S1 provides porewater concentrations of organic carbon sources from the
343 metabolomic analysis, as measured by NMR, that are known to support methanogenesis.
344 Methylamine was detected at SDRO and NDT3-A (1–2 cm), but those concentrations were
345 below the quantification limit (10 μM). Otherwise, methylamine was below detection (< 3 μM)
346 for all other samples. Similarly, methanol was detected but below quantification at NDT3-A
347 (1–2 cm) but otherwise below detection. Acetate was at a quantifiable level (21 μM) at NDT3-
348 A (1–2 cm) but was otherwise either below quantification (SDRO, 1-2 cm; NDRO, 1-2 cm) or
349 below detection.

350

351 **3.2 AOM from ^{14}C -methane and sulfate reduction from ^{35}S -sulfate**

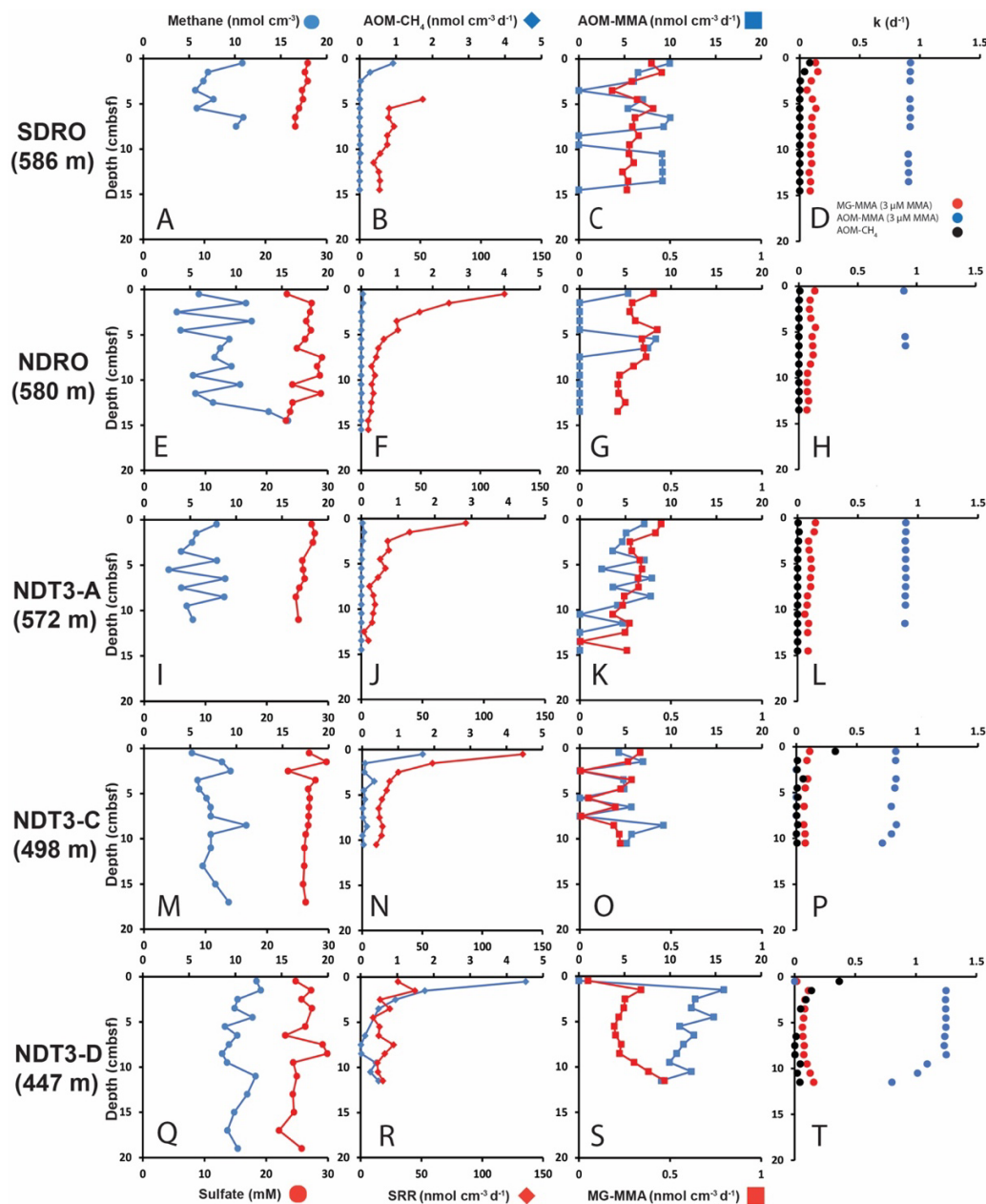
352 Fig. 1B, F, J, N, and R depicts ex-situ rates of AOM- CH_4 and sulfate reduction from
353 the radiotracer incubations with ^{14}C -methane and ^{35}S -sulfate in sediment mini cores,
354 respectively. AOM- CH_4 activity tended to increase with decreasing water depth in the top 5
355 cm of the sediment (from max 0.05 $\text{nmol cm}^{-3} \text{d}^{-1}$ at NDRO to max 4.5 $\text{nmol cm}^{-3} \text{d}^{-1}$ at NDT3-



356 D), while rates were either negligible (SDRO, NDRO, NDT3-A) or $<1 \text{ nmol cm}^{-3} \text{ d}^{-1}$ (NDT3-
357 C, NDT3-D) for depths $>5 \text{ cm}$. Where peaks in AOM were present (SDRO, NDT3-C, NDT3-
358 D) they were always located in the top 0–1 cm sediment layer.

359 Sulfate reduction activity was detected throughout all sediment cores with the highest
360 rates mostly at 0–1 cm, followed by a decrease with increasing sediment depth. The highest
361 individual sulfate reduction peaks were found at NDRO, NDT3-A, and NDT3-C (120, 85 and
362 $133 \text{ nmol cm}^{-3} \text{ d}^{-1}$). At NDT3-D sulfate reduction rates varied between 14 and $45 \text{ nmol cm}^{-3} \text{ d}^{-1}$
363 throughout the core with no clear trend. Note that sulfate reduction data are missing for 0–5
364 cm at SDRO. Here, rates gradually decreased from 52 to $10 \text{ nmol cm}^{-3} \text{ d}^{-1}$ below 5 cm.

365



366

367 **Figure 1.** Depth profiles of biogeochemical parameters in sediment across the depth transect of the Santa Barbara
 368 Basin. A, E, I, M, and Q: sediment methane and porewater sulfate; B, F, J, N, and R: AOM-CH₄ and sulfate
 369 reduction (determined from direct injection of ¹⁴C-CH₄ and ³⁵S-Sulfate, respectively); C, G, K, O, and S:
 370 MMA and MG-MMA (determined from direct injection of ¹⁴C-MMA); D, H, L, P, and T: rate constants for AOM-
 371 CH₄, MG-MMA and AOM-MMA.



372 **3.3 Methanogenesis and AOM from ^{14}C -mono-methylamine**

373 **3.3.1 ^{14}C -MMA recovery from sediment**

374 RF values determined in sediments from NDRO, NDT3-C and D stations (see section
375 2.5.2) were 0.93, 0.84, and 0.75, respectively. They were used to correct MG-MMA rates at
376 each station of the study. Note that no RF values were determined for SDRO or the NDT3-A.
377 We applied RF values from NDRO and NDT3-C, respectively, instead.

378

379 **3.3.2 MG-MMA and AOM-MMA**

380 Fig. 1C, G, K, O, S shows ex-situ rates of MG-MMA and AOM-MMA, assuming a
381 natural MMA concentration of 3 μM (see section 2.5.2). At SDRO, NDRO, and NDT3-A, MG-
382 MMA ranged between 0.27 and 0.45 $\text{nmol cm}^{-3} \text{d}^{-1}$ throughout the sediment core without trend
383 (Fig. 1C, G, and K). At NDT3-C MG-MMA ex-situ rates were lower ranging between 0.007
384 $\text{nmol cm}^{-3} \text{d}^{-1}$ and 0.3 $\text{nmol cm}^{-3} \text{d}^{-1}$ without any pattern (Fig. 1O). At NDT3-D, MG-MMA
385 sharply increased from 0.05 $\text{nmol cm}^{-3} \text{d}^{-1}$ at 0–1cm, to $\sim 0.34 \text{ nmol cm}^{-3} \text{d}^{-1}$ at 1–2 cm. MG-
386 MMA then decreased slightly to $\sim 0.2 \text{ nmol cm}^{-3} \text{d}^{-1}$ between 2 and 9 cm, before increasing to
387 $\sim 0.5 \text{ nmol cm}^{-3} \text{d}^{-1}$ at the bottom of the core (Fig. 1S).

388 AOM-MMA rates were 1 to 2 orders of magnitude higher than MG-MMA rates and 1
389 to 4 orders of magnitude higher than AOM- CH_4 rates (Fig 1C, G, K, O, S). At SDRO, NDRO,
390 NDT3-A, and NDT3-C, AOM-MMA ex-situ rates ranged between 5.3 and 10 $\text{nmol cm}^{-3} \text{d}^{-1}$
391 (unless zero) with no trend (Fig 1C, G, K, and O). At NDT3-D, AOM-MMA rates decreased
392 from 15.9 $\text{nmol cm}^{-3} \text{d}^{-1}$ at 1–2 cm to 9 $\text{nmol cm}^{-3} \text{d}^{-1}$ at 11–12 cm (Fig. 1S). At all stations,
393 some sediment intervals showed no biological net AOM-MMA activity (Fig 1C, G, K, O, S).
394 In these sediment intervals, the ^{14}C -TIC activity was statistically not different from the average
395 plus the standard deviation of the killed control samples.

396

397 **3.4 Rate constants for MG-MMA, AOM-MMA and AOM- CH_4**



398 Fig. 1D, H, L, P, and T show the rate constants (k) for MG-MMA, AOM-MMA and
399 AOM-CH₄ for the comparison of relative radiotracer turnover. At all stations, MG-MMA rate
400 constants were between 0.01 and 0.15 d⁻¹. AOM-CH₄ rate constants ranged between 0.0009 d⁻¹
401 and 0.3 d⁻¹. Rate constants for AOM-MMA, however, were considerably higher than MG-
402 MMA and AOM-CH₄ with values ranging between 0.7 and 1.2 d⁻¹. Most rate constants
403 remained constant over depth, with the exemption of AOM-MMA at station NDT3-C and D
404 (Fig. 1P and T), which showed a steady decrease below 9 cm.



405 4. Discussion

406

407 4.1. Evidence of cryptic methane cycling

408 The aim of the present study was to check for the existence of cryptic methane cycling
409 in SBB surface sediments by presenting evidence for the concurrent activity of sulfate
410 reduction, AOM, and methanogenesis through radiotracer incubations (^{35}S - SO_4^{2-} , ^{14}C - CH_4 ,
411 and ^{14}C -MMA, respectively). Our study confirmed indeed that the three processes co-exist at
412 all investigated stations (Fig. 1). The most prominent concurrent metabolic activity was evident
413 from activity peaks near the sediment-water interface at station NDT3-C (Fig. 1N and O). We
414 suggest the concurrent peaking was stimulated by the availability of fresh, i.e., recently
415 deposited, organic matter coinciding with low oxygen concentrations in the bottom water
416 (Table 1). Fresh organic material likely provided a source for both organoclastic sulfate
417 reduction and methylotrophic methanogenesis, and indirectly (i.e., linked to the methane
418 produced) for AOM coupled to either nitrate, iron, or sulfate reduction. Low oxygen
419 concentrations offered favourable conditions for anaerobic processes in the surface sediment.
420 At the remaining stations (SDRO, NDRO, SDT3-A, SDT3-D; Fig. 1), metabolic activity of all
421 three processes was also confirmed near the sediment surface (with the exemption of the
422 missing data for sulfate reduction at SDRO), but they not always depicted rate peaks
423 (particularly not for AOM- CH_4).

424 Methane detected in the sulfate-rich sediment (Fig. 1A, E, I, M, Q) was likely produced
425 by methylotrophic methanogenesis utilizing non-competitive substrates within the sulfate-
426 reducing zone (Oremland and Taylor, 1978; King et al., 1983; Maltby et al., 2016; Maltby et
427 al., 2018; Reeburgh, 2007), which is also indicated by the production of methane from our ^{14}C -
428 MMA incubations. It is interesting to note that methane concentrations remained relatively
429 constant around 5 to 12 μM while AOM- CH_4 tended to increase with decreasing water depth.
430 This pattern suggests that the threshold partial pressure of methane (the Michaelis constant K_m)



431 of AOM remained at steady state between AOM and methanogenesis (compare, e.g., with
432 Conrad 1999).

433 The finding of relatively constant methane concentrations in surface sediments is
434 against the general view that methane concentrations above the sulfate-methane transition zone
435 show a linear, diffusion-controlled decline towards the sediment-water interface, where
436 methane escapes into the water column (Reeburgh, 2007). We argue that the non-linear
437 methane trends we observe in the present study is an indication for simultaneous methane
438 production and consumption, i.e., cryptic methane cycling, as evident from our radiotracer
439 experiments.

440 As methanogenesis activity showed considerable activity even at the sediment-water
441 interface (0-1 cm) at all stations, aside from station NDT3-D (Fig. 1C, G, K, O, S), it is
442 conceivable that some methane could diffuse into the water column where it may be oxidized
443 by either aerobic or anaerobic oxidation processes (depending on the presence or absence of
444 oxygen, respectively) before emission into the atmosphere (Reeburgh, 2007). However,
445 benthic chamber incubations at the SBB stations did not indicate a release of methane into the
446 water column (Fig. S1), emphasizing the importance of cryptic methane cycling for preventing
447 the build-up of methane in the surface sediment and its emission into the water column.

448

449 ***4.2. Rapid turnover of metabolic substrates***

450 Natural porewater MMA concentrations were mostly below detection ($<3 \mu\text{M}$);
451 however, in porewater close to the sediment-water interface of SDRO and NDT3-A, MMA
452 was detected but below the quantification limit ($<10 \mu\text{M}$) (Table S1). Although we are unable
453 to report definitive MMA concentrations, we can bracket the MMA concentrations in a range
454 between 3 and $10 \mu\text{M}$. The bracketed MMA concentrations are about 1 to 2 orders of magnitude
455 higher than what has been reported from interstitial porewater at other locations. For example,
456 studies of sediment porewater off the coast of Peru found MMA concentrations to be ~ 0.15



457 μM (Wang and Lee, 1990). Similarly, in sediment porewater collected from Buzzards Bay,
458 Massachusetts and in the Eastern Tropical North Pacific Ocean, porewater MMA
459 concentrations were either present at trace amounts or below detection limit ($<0.05 \text{ nmol g dry}$
460 wt^{-1}) (Lee and Olson, 1984). Detectable but low methylamine concentrations in the porewater
461 found in our study could imply that methylamines are rapidly consumed by microbiological
462 processes and/or removed from the porewater through binding to minerals (Wang and Lee,
463 1990; Wang and Lee, 1993; Xiao et al., 2022). Our study provided support for both hypotheses
464 as we detected the biological potential for MMA consumption via radiotracer (^{14}C -MMA)
465 experiments (Fig. 1) and detected the binding of 7-25% the injected ^{14}C -MMA to sediment (see
466 3.3.1).

467 Porewater methanol concentrations in the present study were also mainly below
468 detection, except for one sample, where it was not quantifiable (NDT3-A, 1–2 cm; Table S1).
469 In the marine environment, methanol is known to be a non-competitive substrate for
470 methanogenesis (King et al., 1983; Oremland and Taylor, 1978). However, a recent study
471 demonstrated that methanol is a carbon source for a wide variety of metabolisms, including
472 sulfate-reducing and denitrifying bacteria, as well as aerobic and anaerobic methylotrophs
473 (Fischer et al., 2021), which could all be present in the SBB sediments keeping methanol
474 concentrations low. Acetate was also detected in the metabolomic analysis but mostly below
475 quantification (except NDT3-A, 1–2 cm; Table S1). Acetate is formed through fermentation
476 reactions or through homoacetogenesis (Jørgensen, 2000; Ragsdale and Pierce, 2008). It is a
477 favourable food source for many bacteria and archaea such as sulfate reducers and
478 methanogens (Jørgensen, 2000; Conrad, 2020), which would explain its low concentration in
479 the SBB sediments. Low concentrations of the abovementioned metabolites are likely
480 signatures of rapid metabolic turnover, similar to what has been described for microbial
481 utilization of hydrogen in sediment (Conrad, 1999; Hoehler et al., 2001). In this situation,



482 metabolites would be kept at a steady-state concentration close to the thermodynamic
483 equilibrium of the respective consumers.

484

485 ***4.3. Competitive methylamine turnover by non-methanogenic pathways***

486 Large disparities were found between AOM rates determined from the direct injection
487 of $^{14}\text{C-CH}_4$ (i.e., AOM- CH_4) and AOM determined from the production of $^{14}\text{C-TIC}$ in the $^{14}\text{C-}$
488 MMA incubations (i.e., AOM-MMA). AOM- CH_4 was roughly 1-2 orders of magnitude lower
489 compared AOM-MMA (compare Fig. 1 B/C, F/G, J/K, N/O, R/S), indicating that AOM rates
490 determined via $^{14}\text{C-MMA}$ incubations were overestimated. We hypothesize that this disparity
491 is the result of the direct conversion of $^{14}\text{C-MMA}$ to $^{14}\text{C-TIC}$ by processes other than AOM
492 coupled to MG-MMA. Any process converting $^{14}\text{C-MMA}$ directly to $^{14}\text{C-TIC}$ would inflate
493 the rate constant only slightly for MG-MMA, but dramatically for AOM-MMA (see Eq. 8, 9,
494 and 10). Fig. 1D, H, L, P, and T confirm that the rate constants for AOM-MMA are 1 to 2
495 orders of magnitude higher compared to AOM- CH_4 and MG-MMA. The difference in rate
496 constants strongly suggests that the $^{14}\text{C-TIC}$ detected in the analysis of samples incubated with
497 $^{14}\text{C-MMA}$ must result not only from AOM involved in the cryptic methane cycle but also from
498 direct methylamine oxidation by a different anaerobic methylotrophic metabolism that could
499 not be disambiguated using the adapted radiotracer method.

500 Methylamines are the simplest alkylated amine derived from the degradation of choline
501 and betaine found in plant and phytoplankton biomass (Oren, 1990; Taubert et al., 2017). The
502 molecules are ubiquitously found in saline and hypersaline conditions in the marine
503 environment (Zhuang et al., 2016; Zhuang et al., 2017; Mausz and Chen, 2019). The
504 importance of methylamine as a nitrogen and carbon source for microbes to build biomass has
505 been well documented (Taubert et al., 2017; Capone et al., 2008; Anthony, 1975; Mausz and
506 Chen, 2019). Methylamines can be metabolized by aerobic methylotrophic bacteria (Taubert
507 et al., 2017; Chistoserdova, 2015; Hanson and Hanson, 1996) and by methylotrophic



508 methanogens anaerobically (Chistoserdova, 2015; Thauer, 1998). Here we hypothesize that, in
509 addition to methylotrophic methanogenesis, sulfate reduction was involved in MMA
510 consumption in surface sediment of the SBB.

511 Recent literature does implicate anaerobic methylamine oxidation by sulfate reduction.
512 For example, Cadena et al. (2018) performed in vitro incubations with microbial mats collected
513 from a hypersaline environment with various competitive and non-competitive substrates
514 including tri-methylamine. Microbial mats incubated with trimethylamine stimulated
515 considerable methane production; but after 20 days, H₂S began to accumulate and plateaued
516 after 40 days, suggesting that trimethylamine is not exclusively shuttled to methylotrophic
517 methanogenesis. The molecular data reported in Cadena et al. (2018), however, could not
518 identify a particular group of sulfate-reducing bacteria that proliferated by the addition of
519 trimethylamine. Instead, their molecular data suggested potentially other, non-sulfate reducing
520 bacteria, such as those in the family *Flavobacteriaceae* to be responsible for trimethylamine
521 turnover.

522 Zhuang et al., (2019) investigated heterotrophic metabolisms of C1 and C2 low
523 molecular weight compounds in anoxic sediment collected in the Gulf of Mexico. Sediment
524 was incubated with a variety of ¹⁴C radiotracers alone and in combination with molybdate, a
525 known sulfate reducer inhibitor, to elucidate the metabolic turnover of low molecular weight
526 compounds, including ¹⁴C-labeled trimethylamine. Their results showed that although
527 methylamines did stimulate methane production, radiotracer incubations with molybdate and
528 methylamine demonstrated the inhibition of direct oxidation of ¹⁴C-methylamine to ¹⁴C-CO₂,
529 suggesting that methylamines were simultaneously oxidized to inorganic carbon by non-
530 methanogenic microorganisms. This finding further suggests a competition between
531 methanogens and sulfate-reducing bacteria for methylamine; however, the authors could not
532 rule out AOM as a potential contributor to the inorganic carbon pool.



533 Kivenson et al., (2021) discovered dual genetic code expansion in sulfate-reducing
534 bacteria from sediment within a deep-sea industrial waste dumpsite in the San Pedro Basin,
535 California, which potentially allows the metabolization of trimethylamine. The authors
536 expanded their study to revisit metagenomic and metatranscriptomic data collected from the
537 Baltic Sea and in the Columbia River Estuary and found expression of trimethylamine
538 methyltransferase in Deltaproteobacteria. This result suggested that a trimethylamine
539 metabolism does exist in sulfate-reducing bacteria which was enabled by the utilization of
540 genetic code expansion. Furthermore, the results also suggest that trimethylamine could be the
541 subject of competition between sulfate-reducing bacteria and methylotrophic methanogens.

542 Although the evidence of sulfate-reducing bacteria playing a larger role in methylamine
543 utilization is growing, there are other methylotrophic microorganisms in anaerobic settings that
544 could also be responsible for degrading methylamines. De Anda et al. (2021) discovered and
545 classified a new phylum called Brockarchaeota. The study reconstructed archaeal metagenome-
546 assembled genomes from sediment near hydrothermal vent systems in the Guaymas Basin,
547 Gulf of California, Mexico. Their findings showed that some Brockarchaeota are capable of
548 assimilating trimethylamines, by way of the tetrahydrofolate methyl branch of the Wood-
549 Ljunghal pathway and the reductive glycine pathway, bypassing methane production in anoxic
550 sediment.

551 Farag et al. (2021) found genomic evidence of a novel Asgard Phylum called
552 *Sifarchaeota* in deep marine sediment off the coast of Costa Rica. The study used comparative
553 genomics to show a cluster, *Candidatus* Odinarchaeota within the *Sifarchaeota* Phylum, which
554 contains genes encoding for an incomplete methanogenesis pathway that is coupled to the
555 carbonyl branch of the Wood-Ljunghal pathway. The results suggest that this cluster could be
556 involved with utilizing methylamines. The *Sifarchaeota* metagenome-assembled genomes
557 results found genes for nitrite reductase and sulfate adenylyltransferase and phosphoadenosine
558 phosphosulfate reductase, indicating *Sifarchaeota* could perform nitrite and sulfate reduction.



559 But their study did not directly link nitrite and sulfate reduction to the utilization of
560 methylamines by *Sifarchaeota*.

561 Molecular analysis was not performed in the present study; therefore, we are unable to
562 directly link sulfate-reducing or any other heterotrophic bacteria to the direct anaerobic
563 oxidation of methylamine in the SBB. Future work should combine available geochemical and
564 molecular tools to piece together the complexity of metabolisms involved with methylamine
565 turnover and how it may affect the cryptic methane cycle. We note that there appears to be a
566 growing paradigm shift in the understanding of the utilization of non-competitive substrates in
567 anoxic sediment by sulfate-reducing bacteria and methylotrophic methanogens (including
568 other supposedly non-competitive methanogenic substrates like methanol (Sousa et al., 2018;
569 Fischer et al., 2021)). Apparently, methanogens are in fact able to convert these substrates into
570 methane in the presence of their competitors. Which factors provide them this capability should
571 be the subject of future research.

572

573 ***4.4. Implications for cryptic methane cycling in SBB***

574 The SBB is known to have a network of hydrocarbon cold seeps, where methane and
575 other hydrocarbons are released from the lithosphere into the hydro- and atmosphere either
576 perennially or continuously (Hornafius et al., 1999; Leifer et al., 2010; Boles et al., 2004). The
577 migration of methane and other hydrocarbons vertically into the hydrosphere occur along
578 channels that are focused and permeable, such as fault lines and fractures (Moretti, 1998;
579 Smeraglia et al., 2022). Local tectonics and earthquakes could create new fault lines or fractures
580 that reshape or redisperse less permeable sediments, which may open or close migration
581 pathways for hydrocarbons, including methane (Smeraglia et al., 2022). In fact it has been
582 shown that hydrocarbons move much more efficiently through faults when the region in
583 question is seismically active on time scales <100000 yrs (Moretti, 1998). Given the current
584 and historical seismic activity (Probabilities, 1995) and faulting (Boles et al., 2004) within and



585 surrounding the SBB, it is conceivable that hydrocarbon seep patterns and seepage pathways
586 could also shift over time. A potential consequence of this shifting in the SBB is that methane
587 seepage could spontaneously flow through prior non-seep surface sediment. The fate of this
588 methane would then fall on the methanotrophic communities that are part of the cryptic
589 methane cycle. However, it is not well understood how quickly anaerobic methanotrophs could
590 handle this shift due to their extremely slow growth rates (Knittel and Boetius, 2009; Wilfert
591 et al., 2015; Nauhaus et al., 2007; Dale et al., 2008a). After gaining a better understanding of
592 cryptic methane cycling in the SBB presented in this study, a hypothesis worth testing in future
593 studies is whether cryptic methane cycling based on methylotrophic methanogenesis primes
594 surface sediments to respond faster to increases in methane transport through the sediment.



595 **5. Conclusions**

596 In the present study, we set about to find evidence of cryptic methane cycling in the
597 sulfate-reduction zone of sediment along a depth transect in the oxygen-deficient SBB using a
598 variety of biogeochemical analytics. We found that, within the top 10-20 cm, low methane
599 concentrations were present within sulfate-rich sediment and in the presence of active sulfate
600 reduction. The low methane concentrations were attributed to the balance between
601 methylotrophic methanogenesis and subsequent consumption of the produced methane by
602 AOM. Our results therefore provide strong evidence of cryptic methane cycling in the SBB.
603 We conclude that this important, yet overlooked, process maintains low methane
604 concentrations in surface sediments of this OMZ, and future work should consider cryptic
605 methane cycling in other OMZ's to better constrain carbon cycling in these expanding marine
606 environments.

607 Our radiotracer analyses further indicated microbial activity that oxidizes
608 monomethylamine directly to CO₂ thereby bypassing methane production. Based off the sulfate
609 reduction activity and methylamine consumption to CO₂ detected in this study and the
610 metagenomic clues presented in the literature, we hypothesize that sulfate reduction may also
611 be supported by methylamines. Our study highlights the metabolic complexity and versatility
612 of anoxic marine sediment near the sediment-water interface within the SBB. Future work
613 should consider how methylamines are consumed by different groups of bacteria and archaea,
614 how methylamine utility by other anaerobic methylotrophs affects the cryptic methane cycle
615 and evaluate if potential environmental changes affect the cryptic methane cycle activity.

616



617 **Data Availability Statement**

618 Porewater sulfate concentrations and sulfate reduction rates are accessible through the
619 Biological & Chemical Oceanography Data Management Office (BCO-DMO) under the
620 following DOI's:

621 http://dmoserv3.bco-dmo.org/jg/serv/BCO-DMO/BASIN/porewater_geochemistry.html0,

622 http://dmoserv3.bco-dmo.org/jg/serv/BCO-DMO/BASIN/sediment_parameters.html0,

623 http://dmoserv3.bco-dmo.org/jg/serv/BCO-DMO/BASIN/microbial_activity.html0.

624 Sediment methane concentrations and rates and rate constant data of AOM and methanogenesis
625 can be found in the supplementary material Table S2.

626

627 **Author Contributions**

628 SK and TT designed the study; SK, JL, DY, DR, DH, QQ, FW, and FJ performed experiments
629 and made measurements; SK, JL, DY, DR, DH, QQ, FW, FJ, DV, and TT analysed the data;
630 SK and TT wrote the manuscript draft with input from all co-authors.

631

632 **Competing Interests**

633 Some authors are members of the editorial board of Biogeoscience. The peer-review process
634 was guided by an independent editor, and the authors have also no other competing interests to
635 declare.

636 **Acknowledgements**

637 We thank the captain and crew of R/V Atlantis, the crew of ROV Jason, the crew of AUV
638 Sentry, and the science party of the research cruise AT42-19 for their technical and logistical
639 support. This work was supported by the National Science Foundation NSF Award NO.: EAR-
640 1852912, OCE-1829981 (to TT), and OCE-1830033 (to DV).

641



642 **References**

643

644 Anthony, C.: The biochemistry of methylotrophic micro-organisms, *Science Progress* (1933-),
645 167-206, 1975.

646 Arndt, S., Lange, C. B., and Berger, W. H.: Climatically controlled marker layers in Santa
647 Barbara Basin sediments and fine-scale core-to-core correlation, *Limnology and*
648 *Oceanography*, 35, 165-173, 1990.

649 Barnes, R. and Goldberg, E.: Methane production and consumption in anoxic marine
650 sediments, *Geology*, 4, 297-300, 1976.

651 Beulig, F., Røy, H., McGlynn, S. E., and Jørgensen, B. B.: Cryptic CH₄ cycling in the sulfate-
652 methane transition of marine sediments apparently mediated by ANME-1 archaea,
653 *The ISME journal*, <https://doi.org/10.1038/s41396-41018-40273-z>, 2018.

654 Boetius, A., Ravensschlag, K., Schubert, C. J., Rickert, D., Widdel, F., Giesecke, A., Amann, R.,
655 Jørgensen, B. B., Witte, U., and Pfannkuche, O.: A marine microbial consortium
656 apparently mediating anaerobic oxidation of methane, *Nature*, 407, 623-626, 2000.

657 Boles, J. R., Eichhubl, P., Garven, G., and Chen, J.: Evolution of a hydrocarbon migration
658 pathway along basin-bounding faults: Evidence from fault cement, *AAPG bulletin*, 88,
659 947-970, 2004.

660 Cadena, S., García-Maldonado, J. Q., López-Lozano, N. E., and Cervantes, F. J.: Methanogenic
661 and sulfate-reducing activities in a hypersaline microbial mat and associated
662 microbial diversity, *Microbial ecology*, 75, 930-940, 2018.

663 Canfield, D. E. and Kraft, B.: The 'oxygen' in oxygen minimum zones, *Environmental*
664 *Microbiology*, 24, 5332-5344, 2022.

665 Capone, D. G., Bronk, D. A., Mulholland, M. R., and Carpenter, E. J.: Nitrogen in the marine
666 environment, Elsevier2008.

667 Chistoserdova, L.: Methylotrophs in natural habitats: current insights through
668 metagenomics, *Applied microbiology and biotechnology*, 99, 5763-5779, 2015.

669 Conrad, R.: Contribution of hydrogen to methane production and control of hydrogen
670 concentrations in methanogenic soils and sediments, *FEMS microbiology Ecology*,
671 28, 193-202, 1999.

672 Conrad, R.: Importance of hydrogenotrophic, acetoclastic and methylotrophic
673 methanogenesis for methane production in terrestrial, aquatic and other anoxic
674 environments: a mini review, *Pedosphere*, 30, 25-39, 2020.

675 Dale, A. W., Van Cappellen, P., Aguilera, D., and Regnier, P.: Methane efflux from marine
676 sediments in passive and active margins: Estimations from bioenergetic reaction-
677 transport simulations, *Earth and Planetary Science Letters*, 265, 329-344, 2008a.



- 678 Dale, A. W., Regnier, P., Knab, N. J., Jørgensen, B. B., and Van Cappellen, P.: Anaerobic
679 oxidation of methane (AOM) in marine sediments from the Skagerrak (Denmark): II.
680 Reaction-transport modeling, *Geochim. Cosmochim. Acta*, 72, 2880-2894, 2008b.
- 681 Dale, A. W., Sommer, S., Lomnitz, U., Montes, I., Treude, T., Liebetrau, V., Gier, J., Hensen,
682 C., Dengler, M., Stolpovsky, K., Bryant, L. D., and Wallmann, K.: Organic carbon
683 production, mineralisation and preservation on the Peruvian margin, *Biogeosciences*,
684 12, 1537-1559, 2015.
- 685 De Anda, V., Chen, L.-X., Dombrowski, N., Hua, Z.-S., Jiang, H.-C., Banfield, J. F., Li, W.-J., and
686 Baker, B. J.: Brockarchaeota, a novel archaeal phylum with unique and versatile
687 carbon cycling pathways, *Nature communications*, 12, 1-12, 2021.
- 688 Farag, I. F., Zhao, R., and Biddle, J. F.: "Sifarchaeota," a Novel Asgard Phylum from Costa
689 Rican Sediment Capable of Polysaccharide Degradation and Anaerobic
690 Methyloctrophy, *Applied and environmental microbiology*, 87, e02584-02520, 2021.
- 691 Ferdelman, T. G., Lee, C., Pantoja, S., Harder, J., Bebout, B. M., and Fossing, H.: Sulfate
692 reduction and methanogenesis in a Thioploca-dominated sediment off the coast of
693 Chile, *Geochimica et Cosmochimica Acta*, 61, 3065-3079, 1997.
- 694 Fernandes, S., Mandal, S., Sivan, K., Peketi, A., and Mazumdar, A.: Biogeochemistry of
695 Marine Oxygen Minimum Zones with Special Emphasis on the Northern Indian
696 Ocean, *Systems Biogeochemistry of Major Marine Biomes*, 1-25, 2022.
- 697 Fischer, P. Q., Sánchez-Andrea, I., Stams, A. J., Villanueva, L., and Sousa, D. Z.: Anaerobic
698 microbial methanol conversion in marine sediments, *Environmental microbiology*,
699 23, 1348-1362, 2021.
- 700 Gibb, S. W., Mantoura, R. F. C., Liss, P. S., and Barlow, R. G.: Distributions and
701 biogeochemistries of methylamines and ammonium in the Arabian Sea, *Deep Sea
702 Research Part II: Topical Studies in Oceanography*, 46, 593-615, 1999.
- 703 Hanson, R. S. and Hanson, T. E.: Methanotrophic bacteria, *Microbiol. Rev.*, 60, 439-471,
704 1996.
- 705 Helly, J. J. and Levin, L. A.: Global distribution of naturally occurring marine hypoxia on
706 continental margins, *Deep Sea Research Part I: Oceanographic Research Papers*, 51,
707 1159-1168, 2004.
- 708 Hinrichs, K.-U. and Boetius, A.: The anaerobic oxidation of methane: new insights in
709 microbial ecology and biogeochemistry, in: *Ocean Margin Systems*, edited by: Wefer,
710 G., Billett, D., Hebbeln, D., Jørgensen, B. B., Schlüter, M., and Van Weering, T.,
711 Springer-Verlag, Berlin, 457-477, 2002.



- 712 Hoehler, T. M., Alperin, M. J., Albert, D. B., and Martens, C. S.: Apparent minimum free
713 energy requirements for methanogenic Archaea and sulfate-reducing bacteria in an
714 anoxic marine sediment, *FEMS Microbiol. Ecol.*, 38, 33-41, 2001.
- 715 Hornafius, J. S., Quigley, D., and Luyendyk, B. P.: The world's most spectacular marine
716 hydrocarbon seeps (Coal Oil Point, Santa Barbara Channel, California): Quantification
717 of emissions, *Journal of Geophysical Research: Oceans*, 104, 20703-20711, 1999.
- 718 Joye, S. B., Boetius, A., Orcutt, B. N., Montoya, J. P., Schulz, H. N., Erickson, M. J., and Logo,
719 S. K.: The anaerobic oxidation of methane and sulfate reduction in sediments from
720 Gulf of Mexico cold seeps, *Chem. Geol.*, 205, 219-238, 2004.
- 721 Jørgensen, B. B.: A comparison of methods for the quantification of bacterial sulphate
722 reduction in coastal marine sediments: I. Measurements with radiotracer
723 techniques, *Geomicrobiol. J.*, 1, 11-27, 1978.
- 724 Jørgensen, B. B.: Bacteria and marine biogeochemistry, in: *Marine biogeochemistry*, edited
725 by: Schulz, H. D., and Zabel, M., Springer Verlag, Berlin, 173-201, 2000.
- 726 Kallmeyer, J., Ferdelman, T. G., Weber, A., Fossing, H., and Jørgensen, B. B.: A cold
727 chromium distillation procedure for radiolabeled sulfide applied to sulfate reduction
728 measurements, *Limnol. Oceanogr. Methods*, 2, 171-180, 2004.
- 729 King, G., Klug, M. J., and Lovley, D. R.: Metabolism of acetate, methanol, and methylated
730 amines in intertidal sediments of Lowes Cove, Maine, 45, 1848-1853, 1983.
- 731 Kivenson, V., Paul, B. G., and Valentine, D. L.: An ecological basis for dual genetic code
732 expansion in marine deltaproteobacteria, *Frontiers in microbiology*, 1545, 2021.
- 733 Knittel, K. and Boetius, A.: Anaerobic oxidation of methane: progress with an unknown
734 process, *Annu. Rev. Microbiol.*, 63, 311-334, 2009.
- 735 Kononets, M., Tengberg, A., Nilsson, M., Ekeröth, N., Hylén, A., Robertson, E. K., Van De
736 Velde, S., Bonaglia, S., Rütting, T., and Blomqvist, S.: In situ incubations with the
737 Gothenburg benthic chamber landers: Applications and quality control, *Journal of*
738 *Marine Systems*, 214, 103475, 2021.
- 739 Krause, S. J. and Treude, T.: Deciphering cryptic methane cycling: Coupling of
740 methylotrophic methanogenesis and anaerobic oxidation of methane in hypersaline
741 coastal wetland sediment, *Geochimica et Cosmochimica Acta*, 302, 160-174, 2021.
- 742 Kristjansson, J. K., Schönheit, P., and Thauer, R. K.: Different K_s values for hydrogen of
743 methanogenic bacteria and sulfate reducing bacteria: an explanation for the
744 apparent inhibition of methanogenesis by sulfate, *Arch. Microbiol.*, 131, 278-282,
745 1982.
- 746 Lee, C. and Olson, B. L.: Dissolved, exchangeable and bound aliphatic amines in marine
747 sediments: initial results, *Organic Geochemistry*, 6, 259-263, 1984.



- 748 Leifer, I., Kamerling, M. J., Luyendyk, B. P., and Wilson, D. S.: Geologic control of natural
749 marine hydrocarbon seep emissions, Coal Oil Point seep field, California, *Geo-Marine*
750 *Letters*, 30, 331-338, 2010.
- 751 Levin, L.: Oxygen minimum zone benthos: Adaptation and community response to hypoxia,
752 *Oceanogr. Mar. Biol. Ann. Rev.*, 41, 1-45, 2003.
- 753 Levin, L. A. E., W., Gooday, A. J., Jorissen, F., Middelburg, J. J., Naqvi, S. W. A., Neira, C., and
754 Rabalais, N. N. Z., J.: Effects of natural and human-induced hypoxia on coastal
755 benthos, *Biogeosciences*, 6, 2063–2098, 2009.
- 756 Lovley, D. R. and Klug, M. J.: Model for the distribution of sulfate reduction and
757 methanogenesis in freshwater sediments, *Geochim. Cosmochim. Acta*, 50, 11-18,
758 1986.
- 759 Lyu, Z., Shao, N., Akinyemi, T., and Whitman, W. B.: Methanogenesis, *Current Biology*, 28,
760 R727-R732, 2018.
- 761 Maltby, J., Sommer, S., Dale, A. W., and Treude, T.: Microbial methanogenesis in the sulfate-
762 reducing zone of surface sediments traversing the Peruvian margin, *Biogeosciences*,
763 13, 283–299, 2016.
- 764 Maltby, J., Steinle, L., Löscher, C. R., Bange, H. W., Fischer, M. A., Schmidt, M., and Treude,
765 T.: Microbial methanogenesis in the sulfate-reducing zone of sediments in the
766 Eckernförde Bay, SW Baltic Sea, *Biogeosciences*, 15, 137– 157, 2018.
- 767 Mausz, M. A. and Chen, Y.: Microbiology and ecology of methylated amine metabolism in
768 marine ecosystems, *Current Issues in Molecular Biology*, 33, 133-148, 2019.
- 769 Michaelis, W., Seifert, R., Nauhaus, K., Treude, T., Thiel, V., Blumenberg, M., Knittel, K.,
770 Gieseke, A., Peterknecht, K., Pape, T., Boetius, A., Aman, A., Jørgensen, B. B., Widdel,
771 F., Peckmann, J., Pimenov, N. V., and Gulin, M.: Microbial reefs in the Black Sea
772 fueled by anaerobic oxidation of methane, *Science*, 297, 1013-1015, 2002.
- 773 Middelburg, J. J. and Levin, L. A.: Coastal hypoxia and sediment biogeochemistry,
774 *Biogeosciences*, 6, 1273-1293, 2009.
- 775 Moretti, I.: The role of faults in hydrocarbon migration, *Petroleum Geoscience*, 4, 81-94,
776 1998.
- 777 Nauhaus, K., Albrecht, M., Elvert, M., Boetius, A., and Widdel, F.: In vitro cell growth of
778 marine archaeal-bacterial consortia during anaerobic oxidation of methane with
779 sulfate, *Environ. Microbiol.*, 9, 187-196, 2007.
- 780 Oremland, R. S. and Polcin, S.: Methanogenesis and sulfate reduction: competitive and
781 noncompetitive substrates in estuarine sediments, *Appl. Environ. Microbiol.*, 44,
782 1270-1276, 1982.



- 783 Oremland, R. S. and Taylor, B. F.: Sulfate reduction and methanogenesis in marine
784 sediments, *Geochimica et Cosmochimica Acta*, 42, 209-214, 1978.
- 785 Oremland, R. S., Marsh, L. M., and Polcin, S.: Methane production and simultaneous
786 sulphate reduction in anoxic, salt marsh sediments, *Nature*, 296, 143-145, 1982.
- 787 Oren, A.: Formation and breakdown of glycine betaine and trimethylamine in hypersaline
788 environments, *Antonie van Leeuwenhoek*, 58, 291-298, 1990.
- 789 Orphan, V. J., Hinrichs, K.-U., Ussler III, W., Paull, C. K., Tayleur, L. T., Sylva, S. P., Hayes, J. M.,
790 and DeLong, E. F.: Comparative analysis of methane-oxidizing archaea and sulfate-
791 reducing bacteria in anoxic marine sediments, *Appl. Environ. Microbiol.*, 67, 1922-
792 1934, 2001.
- 793 Paulmier, A. and Ruiz-Pino, D.: Oxygen minimum zones (OMZs) in modern ocean, *Progr.*
794 *Oceanog.*, 80, 113-128, 2009.
- 795 Probabilities, W. G. o. C. E.: Seismic hazards in southern California: probable earthquakes,
796 1994 to 2024, *Bulletin of the Seismological Society of America*, 85, 379-439, 1995.
- 797 Qin, Q., Kinnaman, F. S., Gosselin, K. M., Liu, N., Treude, T., and Valentine, D. L.: Seasonality
798 of water column methane oxidation and deoxygenation in a dynamic marine
799 environment, *Geochimica et Cosmochimica Acta*, 336, 219-230, 2022.
- 800 Ragsdale, S. W. and Pierce, E.: Acetogenesis and the Wood–Ljungdahl pathway of CO₂
801 fixation, *Biochimica et Biophysica Acta (BBA)-Proteins and Proteomics*, 1784, 1873-
802 1898, 2008.
- 803 Reeburgh, W. S.: Oceanic methane biogeochemistry, *Chem. Rev.*, 107, 486-513, 2007.
- 804 Reimers, C. E., Ruttenger, K. C., Canfield, D. E., Christiansen, M. B., and Martin, J. B.:
805 Porewater pH and authigenic phases formed in the uppermost sediments of Santa
806 Barbara Basin, *Geochim. Cosmochim. Acta*, 60, 4037-4057, 1996.
- 807 Rullkötter, J.: Organic matter: the driving force for early diagenesis, in: *Marine*
808 *geochemistry*, Springer, 125-168, 2006.
- 809 Schimmelmann, A. and Kastner, M.: Evolutionary changes over the last 1000 years of
810 reduced sulfur phases and organic carbon in varved sediments of the Santa Barbara
811 Basin, California, *Geochimica et Cosmochimica Acta*, 57, 67-78, 1993.
- 812 Sholkovitz, E.: Interstitial water chemistry of the Santa Barbara Basin sediments, *Geochimica*
813 *et Cosmochimica Acta*, 37, 2043-2073, 1973.
- 814 Smeraglia, L., Fabbi, S., Billi, A., Carminati, E., and Cavinato, G. P.: How hydrocarbons move
815 along faults: Evidence from microstructural observations of hydrocarbon-bearing
816 carbonate fault rocks, *Earth and Planetary Science Letters*, 584, 117454, 2022.
- 817 Sousa, D. Z., Visser, M., Van Gelder, A. H., Boeren, S., Pieterse, M. M., Pinkse, M. W.,
818 Verhaert, P. D., Vogt, C., Franke, S., and Kümmel, S.: The deep-subsurface sulfate



- 819 reducer *Desulfotomaculum kuznetsovii* employs two methanol-degrading pathways,
820 *Nature communications*, 9, 1-9, 2018.
- 821 Soutar, A. and Crill, P. A.: Sedimentation and climatic patterns in the Santa Barbara Basin
822 during the 19th and 20th centuries, *Geological Society of America Bulletin*, 88, 1161-
823 1172, 1977.
- 824 Stephenson, M. and Stickland, L. H.: CCVII. Hydrogenase. III. The bacterial formation of
825 methane by the reduction of one-carbon compounds by molecular hydrogen,
826 *Biochem. J.*, 27, 1517–1527, 1933.
- 827 Taubert, M., Grob, C., Howat, A. M., Burns, O. J., Pratscher, J., Jehmlich, N., von Bergen, M.,
828 Richnow, H. H., Chen, Y., and Murrell, J. C.: Methylamine as a nitrogen source for
829 microorganisms from a coastal marine environment, *Environmental microbiology*,
830 19, 2246-2257, 2017.
- 831 Thauer, R. K.: Biochemistry of methanogenesis: a tribute to Marjory Stephenson,
832 *Microbiology*, 144, 2377-2406, 1998.
- 833 Treude, T.: Biogeochemical reactions in marine sediments underlying anoxic water bodies,
834 in: *Anoxia: Paleontological Strategies and Evidence for Eukaryote Survival*, edited by:
835 Altenbach, A., Bernhard, J., and Seckbach, J., *Cellular Origins, Life in Extreme Habitats*
836 *and Astrobiology (COLE) Book Series*, Springer, Dordrecht, 18-38, 2011.
- 837 Treude, T., Krüger, M., Boetius, A., and Jørgensen, B. B.: Environmental control on anaerobic
838 oxidation of methane in the gassy sediments of Eckernförde Bay (German Baltic),
839 *Limnol. Oceanogr.*, 50, 1771-1786, 2005.
- 840 Treude, T., Smith, C. R., Wenzhoefer, F., Carney, E., Bernardino, A. F., Hannides, A. K.,
841 Krueger, M., and Boetius, A.: Biogeochemistry of a deep-sea whale fall: sulfate
842 reduction, sulfide efflux and methanogenesis, *Mar. Ecol. Prog. Ser.*, 382, 1-21, 2009.
- 843 Wang, X.-c. and Lee, C.: The distribution and adsorption behavior of aliphatic amines in
844 marine and lacustrine sediments, *Geochimica et Cosmochimica Acta*, 54, 2759-2774,
845 1990.
- 846 Wang, X.-C. and Lee, C.: Adsorption and desorption of aliphatic amines, amino acids and
847 acetate by clay minerals and marine sediments, *Marine Chemistry*, 44, 1-23, 1993.
- 848 Wang, X.-C. and Lee, C.: Sources and distribution of aliphatic amines in salt marsh sediment,
849 *Organic Geochemistry*, 22, 1005-1021, 1994.
- 850 Wehrmann, L. M., Risgaard-Petersen, N., Schrum, H. N., Walsh, E. A., Huh, Y., Ikehara, M.,
851 Pierre, C., D'Hondt, S., Ferdelman, T. G., and Ravelo, A. C.: Coupled organic and
852 inorganic carbon cycling in the deep seafloor sediment of the northeastern
853 Bering Sea Slope (IODP Exp. 323), *Chemical Geology*, 284, 251-261, 2011.



- 854 Wilfert, P., Krause, S., Liebetrau, V., Schönfeld, J., Haeckel, M., Linke, P., and Treude, T.:
855 Response of anaerobic methanotrophs and benthic foraminifera to 20 years of
856 methane emission from a gas blowout in the North Sea, *Marine and Petroleum*
857 *Geology*, 68, 731-742, 2015.
- 858 Winfrey, M. R. and Ward, D. M.: Substrates for sulfate reduction and methane production
859 in intertidal sediments, *Appl. Environm. Microbiol*, 45, 193-199, 1983.
- 860 Wright, J. J., Konwar, K. M., and Hallam, S. J.: Microbial ecology of expanding oxygen
861 minimum zones, *Nature Reviews Microbiology*, 10, 381-394, 2012.
- 862 Wyrski, K.: The oxygen minima in relation to ocean circulation, *Deep Sea Research and*
863 *Oceanographic Abstracts*, 11-23,
- 864 Xiao, K., Beulig, F., Kjeldsen, K., Jorgensen, B., and Risgaard-Petersen, N.: Concurrent
865 Methane Production and Oxidation in Surface Sediment from Aarhus Bay, Denmark,
866 *Frontiers in Microbiology*, 8, 10.3389/fmicb.2017.01198, 2017.
- 867 Xiao, K., Beulig, F., Roy, H., Jorgensen, B., and Risgaard-Petersen, N.: Methylo-trophic
868 methanogenesis fuels cryptic methane cycling in marine surface sediment,
869 *Limnology and Oceanography*, 63, 1519-1527, 10.1002/lno.10788, 2018.
- 870 Xiao, K.-Q., Moore, O. W., Babakhani, P., Curti, L., and Peacock, C. L.: Mineralogical control
871 on methylo-trophic methanogenesis and implications for cryptic methane cycling in
872 marine surface sediment, *Nature Communications*, 13, 1-9, 2022.
- 873 Zhuang, G.-C., Montgomery, A., and Joye, S. B.: Heterotrophic metabolism of C1 and C2 low
874 molecular weight compounds in northern Gulf of Mexico sediments: Controlling
875 factors and implications for organic carbon degradation, *Geochimica et*
876 *Cosmochimica Acta*, 247, 243-260, 2019.
- 877 Zhuang, G.-C., Elling, F. J., Nigro, L. M., Samarkin, V., Joye, S. B., Teske, A., and Hinrichs, K.-
878 U.: Multiple evidence for methylo-trophic methanogenesis as the dominant
879 methanogenic pathway in hypersaline sediments from the Orca Basin, Gulf of
880 Mexico, *Geochim. Cosmochim. Acta*, 187, 1-20, 2016.
- 881 Zhuang, G.-C., Lin, Y.-S., Bowles, M. W., Heuer, V. B., Lever, M. A., Elvert, M., and Hinrichs,
882 K.-U.: Distribution and isotopic composition of trimethylamine, dimethylsulfide and
883 dimethylsulfoniopropionate in marine sediments, *Mar. Chem.*, 196, 35-46, 2017.
- 884 Zhuang, G.-C., Heuer, V. B., Lazar, C. S., Goldhammer, T., Wendt, J., Samarkin, V. A., Elvert,
885 M., Teske, A. P., Joye, S. B., and Hinrichs, K.-U.: Relative importance of
886 methylo-trophic methanogenesis in sediments of the Western Mediterranean Sea,
887 *Geochim. Cosmochim. Acta*, 224, 2018.
- 888
- 889